Collider Signatures of Minimal Flavor Mixing from Stop Decay Length Measurements

Gudrun Hiller, Jong Soo Kim and Henning Sedello
Institut für Physik, Technische Universität Dortmund, D-44221 Dortmund, Germany

We investigate the prospects to extract supersymmetric couplings from a decay length measurement at the LHC. Specifically, we exploit the opportunity of a light and long-lived stop which is pair-produced through gluinos in association with like-sign top quarks. Any observed finite value of the stop decay length strongly supports models in which flavor is broken in a minimal way solely by the Standard Model Yukawa couplings. We find that a 1 picosecond stop lifetime, dominated by $\tilde{t} \to c\chi^0$ decays, yields macroscopic transverse impact parameters of about 180 microns. If the lightest neutralino is predominantly higgsino or very close in mass to the light stop, the stop lifetime even increases and allows to observe stop tracks and possibly secondary vertices directly. Measuring squark flavor violation with the stop decay length works also with a gravitino LSP if the neutralino is the NLSP. For this case, opportunities from $\tilde{t} \to c\chi^0 \to c\gamma\tilde{G}$ decays for very light gravitinos with mass $\lesssim$ keV are pointed out.

PACS numbers: 14.80.Ly,12.60.Jv,12.90.+b

I. INTRODUCTION

The past decade has brought great advances in the description of quark flavor violation in the Standard Model (SM) in terms of both consistency checks and precision. Together with the constraints from K, D and B meson studies on flavor changing neutral currents (FCNC), this has strong implications: The physics at the TeV-scale cannot contain much more flavor violation than the SM [1]. Intriguing loopholes exist presently, however [2].

A generic framework consistent with current flavor observations is minimal flavor violation (MFV), where the Yukawa matrices are the sole source of flavor breaking, as in the SM. In the context of the minimal supersymmetric standard model (MSSM), MFV predicts highly degenerate first and second generation squarks and their mixing with the third generation to be suppressed by small CKM quark mixing angles V_{ij} of the order $|V_{cb}|, |V_{ts}| \sim 0.04$ (second-third generation) or smaller $|V_{ub}| \sim 0.004$, $|V_{td}| \sim 0.01$ (first-third generation).

Is it possible to directly measure such small flavor changing couplings in squark mixing and support MFV? We pursue here the proposal of Ref. [3] and exploit the opportunity of a light stop whose decay to top quarks is kinematically forbidden. If this stop then decays predominantly via FCNC into charm and the lightest neutralino $\tilde{t} \to c\chi^0$, it has a long life because the coupling between stop and charm is CKM-suppressed as dictated by MFV. (In this work $\tilde{t}$ and χ^0 always denote the lightest stop and neutralino, respectively.) Lifetimes of order picoseconds are possible, and with boost factors $\gamma\beta \sim 1$ [33], this leads to a macroscopic decay length of the order of a few hundred microns. The goal of this work is to analyze the prospects to observe this scenario and extract superpartner MFV couplings at the LHC.

The paper is organized as follows: In Sec. II we briefly review the framework of a light stop in MFV. In Sec. III the collider signatures are worked out. The lightest supersymmetric particle (LSP) does not need to be the χ^0. In Sec. IV we consider the case with a gravitino LSP and the stop or the neutralino being the next lightest supersymmetric particle (NLSP). In Sec. V we summarize and conclude.

II. A LIGHT STOP IN MFV

Our framework is a generic MSSM setting which is MFV and where the lightest stop decays predominantly to charm. (Decays to first generation up quarks are further CKM-suppressed.) Many of the contemporary TeV-scale models are MFV, such as gauge and anomaly mediation and hybrids, *e.g.,* [4], or by construction, the CMSSM and msugra, see, *e.g.,* [5].

Within MFV, all flavor changing effects with squarks and quarks are controlled by the quark Yukawas λ_q and CKM angles [6]. In particular, the $\tilde{t} - c - \chi^0$ coupling Y is parametrically suppressed as [3, 7]

$$Y \propto \lambda_b^2 V_{cb} V_{tb}^* \sim 3 \cdot 10^{-5} \tan\beta^2, \qquad (1)$$

where the higgsino component of the χ^0 receives an additional suppression by the charm Yukawa $\lambda_c \sim 10^{-2}$. The precise value of Y depends on the composition of the stop and the neutralino and, to some extent, on the flavor diagonal properties of the supersymmetry (susy) breaking mechanism. Hence, even further suppressions beyond those from flavor given in Eq. (1) can arise [3].

In models with flavor blind susy breaking at the scale of mediation M, intergenerational squark mixing is radiatively induced at the weak scale m_Z at order $1/(16\pi^2)\ln(m_Z/M)$ times a flavor factor, which for the case of stop-scharm mixing is written in Eq. (1). Since the coupling Y is normalized to an average squark mass squared which also receives logarithmic corrections, the dependence on the scale M gets partially cancelled. There is, however, sensitivity to the relative size of gaugino and flavor-universal scalar masses and trilinear terms.

Note that a small Y is very specific to MFV susy. Other MSSM variants give generically larger values of

the flavor factors, such as $Y \propto \lambda_c$ (flavor anarchy) or $Y \propto V_{cb}\lambda_c$ (alignement [8]).

Stop decays into tops, which would otherwise be a leading channel, can be forbidden by a suitable spectrum

$$\Delta m = m_{\tilde{t}} - m_{\chi^0} < m_t, \tag{2}$$

where $m_{\tilde{t}}, m_{\chi^0}$, and m_t denotes the mass of the lightest stop, the lightest neutralino, and the top quark, respectively.

To also avoid a contamination from four-body decays $\tilde{t} \to b\ell\nu\chi^0$, Δm needs to be lower than the bound given in Eq. (2). The actual value is model-dependent and typically in the range [few$(5-10)$] GeV. This choice is also consistent with the constraints from direct searches [9]. Neglecting the charm mass in kinematical factors, the $\tilde{t} \to c\chi^0$ decay rate is then given as

$$\Gamma = \frac{m_{\tilde{t}} Y^2}{16\pi}\left(1 - \frac{m_{\chi^0}^2}{m_{\tilde{t}}^2}\right)^2 \approx \frac{m_{\tilde{t}} Y^2}{4\pi}\left(\frac{\Delta m}{m_{\tilde{t}}}\right)^2. \tag{3}$$

It is suppressed by the small coupling and mass splitting.

With $m_{\tilde{t}} \sim \mathcal{O}(100)$ GeV and Eqs. (1)-(3), stop lifetimes in the picoseconds range arise. Consequently, the stop hadronizes before decay.

III. $\tilde{t} \to c\chi^0$ COLLIDER SIGNATURES

We work out collider signatures of a light stop decaying to charm and the lightest neutralino within MFV susy. We make a few minimal assumptions on the susy spectrum only: The lighter stop is light, and its mass is not too far away from the one of the lightest neutralino. In addition, we require the mass of the gluino $m_{\tilde{g}}$ to be sufficiently heavy to allow for decays to $\tilde{t}\bar{t}$ and $\tilde{t}^* t$. The masses of all other squarks except for the lighter stop should be sufficiently above $m_{\tilde{g}}$ such that the gluino decays predominantly into these top plus light stop modes.

A. Open stop production

We consider stop production in association with like-sign tops in pp-collisions

$$pp \to \tilde{g}\tilde{g} \to tt\tilde{t}^*\tilde{t}^*, \bar{t}\bar{t}\tilde{t}\tilde{t}. \tag{4}$$

Such processes arise due to the Majorana nature of the gluinos and, unlike the reaction into $t\bar{t}\tilde{t}\tilde{t}^*$-states, have a controlled background [10]. Direct stop pair-production, $pp \to \tilde{t}\tilde{t}^*$, is disfavored despite its large cross section of the order of several hundred pb [11] [34] due to the difficult stop identification from charm jets plus missing energy, *e.g.,* [12, 13]. See, however, [13] for cases if one of the stops decays differently than via FCNCs, and [14]. We will come back to di-stop production in Sec. IV C.

For the numerical analysis we use MadGraph/MadEvent 4.4.23 [15] and independently our own leading order event generator with CTEQ6L1 parton distribution functions [16]. We use for the factorization and renormalization scales $\mu = m_{\tilde{g}}$. With $m_{\tilde{t}} \sim \mathcal{O}(100)$ GeV and $m_{\tilde{g}} = 500$ GeV cross sections of 5 pb for the processes Eq. (4) at the LHC are obtained. The cross section decreases to 0.2 pb for $m_{\tilde{g}} = 1000$ GeV. The dependence on the stop mass is very mild for light stops below the top. Next-to-leading order corrections yield K-factors of $\sim 1.5 - 2$ for di-gluino production at the LHC [17], suggesting similar enhancements for top-associated stop production Eq. (4). For a lower proton-proton center-of-mass energy of 10 TeV, the cross sections for Eq. (4) are reduced by a factor of ~ 0.15 with respect to those in the 14 TeV case.

B. Stop boost and decay length

The stop decay lengths $d_i, i = 1, 2$ are related to the fundamental parameters on average [35] as

$$d_i = \frac{(\gamma\beta)_i}{\Gamma} \approx \frac{4\pi p_i}{(\Delta m Y)^2}, \tag{5}$$

where the p_i denote the magnitudes of the three momenta of the two stops in the laboratory frame. In the second step we used the small mass splitting approximation $\Delta m \ll m_{\tilde{t}}$, see Eq. (3).

A measurement of the decay length can be used to extract $\Delta m Y$ if the stop kinematics is known and to extract Y if the mass splitting is known also. As already stressed, the exact value of Y, within MFV, could tell us something about the composition of the lightest stop and neutralino and the susy breaking mechanism.

For $m_{\tilde{t}} \sim \mathcal{O}(100)$ GeV and $m_{\tilde{g}} \sim (500 - 1000)$ GeV the stops produced at the LHC through Eq. (4) are typically boosted with $\gamma\beta \sim \mathcal{O}(1-10)$, supporting macroscopic decay lengths, see Eq. (3), as

$$d_i \sim 0.5\text{mm}\ \frac{(\gamma\beta)_i}{5}\left(\frac{100\text{GeV}}{m_{\tilde{t}}}\right)\left(\frac{0.05}{\Delta m/m_{\tilde{t}}}\right)^2\left(\frac{10^{-5}}{Y}\right)^2. \tag{6}$$

The boost factors increase for heavier gluinos, however, at the price of fewer events.

We show the distribution of the boost factors of the two stops in Fig. 1 for $m_{\tilde{g}} = 500$ GeV. For the dominant part of the events, both stops have a significant boost: 92% of the events have both $(\gamma\beta)_i > 1$ and are produced in the central region, see Fig. 2. 85% of the events with both $(\gamma\beta)_i > 1$ have $|\eta_i| \leq 2.5$ (η denotes the pseudo-rapidity). As shown in Fig. 3, the stops are also well separated in terms of $|\eta_1 - \eta_2|$ or

$$\delta R = \sqrt{(\eta_1 - \eta_2)^2 + (\phi_1 - \phi_2)^2}, \quad |\phi_1 - \phi_2| \leq \pi, \tag{7}$$

where ϕ_i denote the azimutal angles of the stops in the laboratory frame. In Figs. 1-3 the stops in each event are labeled according to $(\beta\gamma)_1 \geq (\beta\gamma)_2$.

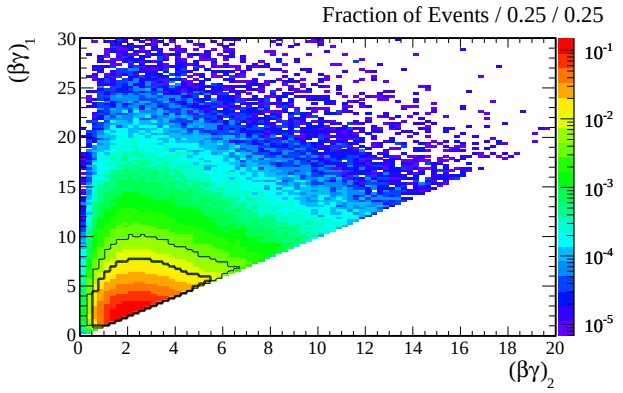

FIG. 1: The stop boost factors at the LHC in processes Eq. (4) for $m_{\tilde{t}} = 100$ GeV and $m_{\tilde{g}} = 500$ GeV. The thick (thin) contour contains 80% (90%) of the events.

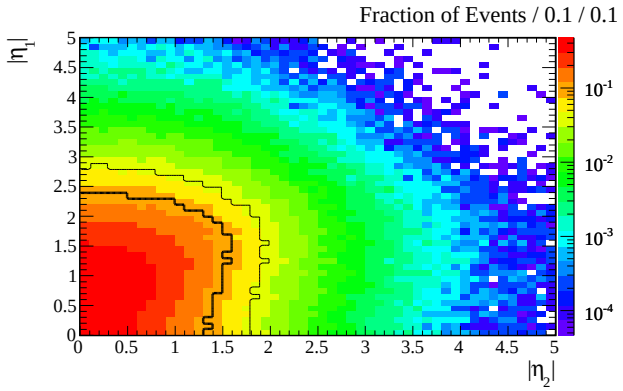

FIG. 2: The pseudo-rapidity distribution of the two stops at the LHC in processes Eq. (4) for $m_{\tilde{t}} = 100$ GeV and $m_{\tilde{g}} = 500$ GeV. In all shown events both stops satisfy $\gamma\beta > 1$. The thick (thin) contour contains 80% (90%) of the events shown.

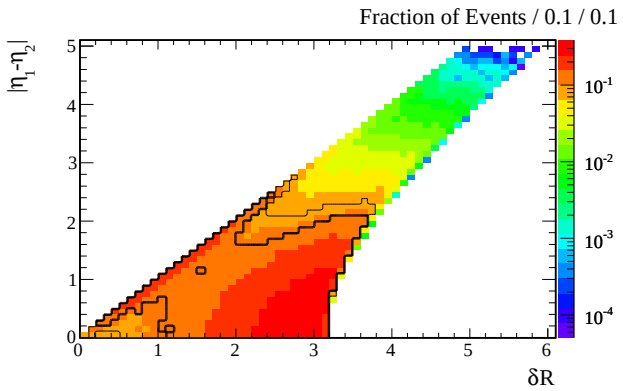

FIG. 3: The transverse separation $|\eta_1 - \eta_2|$ versus δR of the stops at the LHC in processes Eq. (4) for $m_{\tilde{t}} = 100$ GeV and $m_{\tilde{g}} = 500$ GeV. In all shown events the stops satisfy $\gamma\beta > 1$ and $|\eta| < 2.5$. The thick (thin) contour contains 80% (90%) of the events shown.

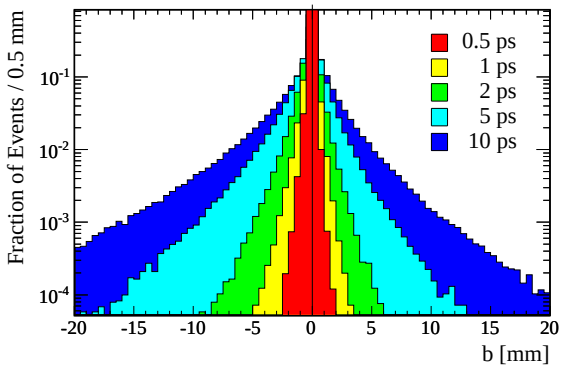

FIG. 4: The distribution of impact parameters b_i in mm at the LHC in processes Eq. (4) for different stop lifetimes. The curves with $b_i > 0 (< 0)$ refer to the stop in each event with larger (smaller) charm p_T.

In a typical scenario the stops will travel distances up to millimeters, see Eq. (6). Hence, the stops will decay before they reach sensible detector material, being away a few cm from the interaction point within the beam pipe [18, 19]. Consequently, we have direct access only to the impact parameters in the transverse plane, b_i, for both stops, obtained from extrapolating the charm trajectories and taking their closest distance with respect to the beam axis. (In our analysis, we neglect bending effects due to magnetic fields.)

The impact parameters constitute lower bounds on the decay lengths, $d_i \geq b_i$. Already an observation of any finite value of b_i strongly supports MFV since other flavor implementations of the MSSM generically yield a promptly decaying stop, see Sec. II.

Even assuming the optimal situation where all relevant masses are known, due to the missing energies, the momenta of the stops – and the individual lifetimes, see Eq. (5) – cannot be reconstructed on an event-by-event basis. We can however obtain information about the stop lifetime from the distribution and moments of impact parameters of the stops.

We show the b_i distribution in Fig. 4 for different values of the stop lifetime $\tau = 0.5, 1, 2, 5$, and 10 ps, corresponding to different values of Y, with all input masses fixed to $m_{\tilde{t}} = 100$ GeV and $m_{\tilde{g}} = 500$ GeV. For a fixed stop lifetime, the dependence of the impact parameter on the mass splitting is negligible as long as it is sufficiently above the charm mass (we used $\Delta m = 5$ GeV for the plot). The reason is that for a relativistic charm quark the angle between the stop and charm momenta in the laboratory frame becomes insensitive to the charm momentum. The two b_i per event are sorted according to the charm transverse momenta p_T: positive (negative) values refer to the charm quark with larger (smaller) p_T. The simulated events show that the distribution is indicative for the stop lifetime.

Numerically, the average impact parameter can be well

approximated as

$$\langle b\rangle \simeq 180\,\mu\text{m}\cdot\left(\frac{\tau}{\text{ps}}\right). \tag{8}$$

The formula is largely insensitive to the stop boost factors, *i.e.,* the gluino and stop mass [36]. The asymmetry between the two impact parameters $(\langle b_1\rangle - \langle b_2\rangle)/(\langle b_1\rangle + \langle b_2\rangle)$ is 24%.

If the stop coupling Y is even further suppressed than in Eq. (1), for instance due to small wino/bino components in the χ^0, the decay lengths may be measured directly. Specifically, inspecting Eq. (6) for

$$\frac{\Delta m}{m_{\tilde t}} Y \lesssim 5\cdot 10^{-8}, \tag{9}$$

decay lengths of a few centimeters and larger arise; hence, the (hadronized) stops produce tracks from interactions with the detector material, see [20]. The appearance of stop tracks is advantageous because more information can be obtained without relying solely on the charm jets.

Very small values of

$$\frac{\Delta m}{m_{\tilde t}} Y \lesssim 4\cdot 10^{-9} \tag{10}$$

yield stops which travel the detector undecayed. Searches from the CDF experiment at the Tevatron have ruled out this scenario for light stops with masses below 249 GeV [21].

C. Stop events

Stops decaying to charm jets and missing energy in association with like-sign tops, Eq. (4), can be searched for in the final states

$$bbjj\ell^+\ell^+ \not{E}_T, \quad \bar b\bar b jj\ell^-\ell^- \not{E}_T, \qquad \ell = e,\mu, \tag{11}$$

requiring leptonically decaying top quarks. As discussed in [10], signals can be separated from the SM and susy backgrounds at the LHC by employing cuts on same-sign isolated lepton pairs, missing transverse energy, $\not{E}_T$, and the transverse momenta of the four (c and b) hardest jets. In our simulation $\not{E}_T$ consists of the two lightest neutralinos and the two neutrinos from the leptonic decays of the top quarks.

In Fig. 5 we show the p_T distributions of the two charm quarks for $m_{\tilde t} = 100$ GeV, $m_{\tilde g} = 500$ GeV, and $\Delta m = 5$ GeV. The charm p_T increases with increasing stop boost, hence, for heavier gluinos and lighter stops. A small stop-neutralino mass splitting supports a stop branching ratio dominated by FCNC, $\mathcal{B}(\tilde t \to c\chi^0) \simeq 1$, and a long stop lifetime, see Eq. (3), but it also makes the charm jets less energetic. The p_T distribution of the charm quarks with lower p_T per event is shown for different values of Δm in Fig. 6. We kept the stop mass fixed, hence, lowered the mass of the lightest neutralino correspondingly. The

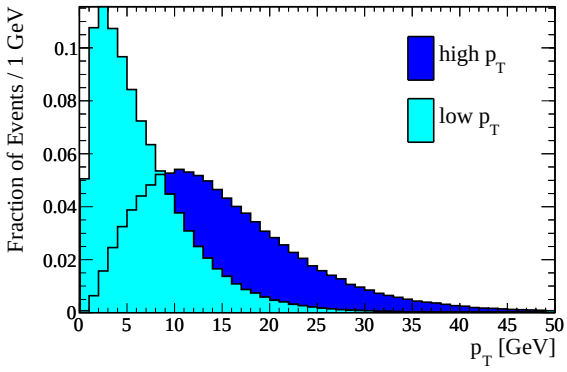

FIG. 5: The p_T distributions of the charm quarks stemming from the decays of light stops produced in processes Eq. (4) for $m_{\tilde t} = 100$ GeV, $m_{\tilde g} = 500$ and $\Delta m = 5$ GeV. The light blue (lighter shaded) histogram corresponds to the charm quarks with per event lower p_T.

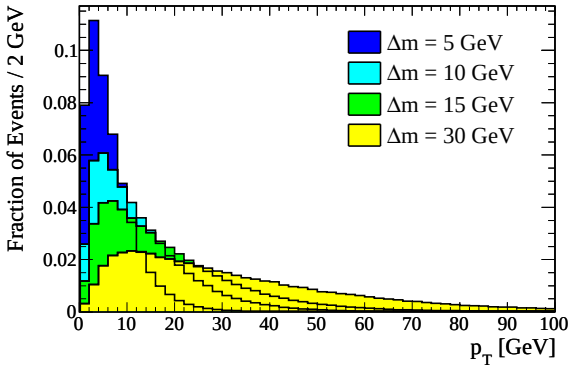

FIG. 6: The p_T distribution of the lower p_T charm quarks stemming from the decays of light stops produced in processes Eq. (4) for $m_{\tilde t} = 100$ GeV, $m_{\tilde g} = 500$ GeV, and different mass splittings Δm.

fraction of events surviving various p_T cuts for different mass splittings is given in Tab. I.

With a factor of $(2/9)^2$ for leptonically (μ or e) decaying top quarks, the expected number of events for an integrated luminosity of $3(10)\,\text{fb}^{-1}$ and $\sigma_{NLO} = 7.5$ pb (for $m_{\tilde t} = 100$ GeV and $m_{\tilde g} = 500$ GeV) is about 1110(3700) times loss due to kinematical cuts and detector effects. From the p_T cuts of 20 GeV for the charged leptons, 50 GeV for each b, and 100 GeV for $\not{E}_T$[10], a reduction factor of 0.42 arises. The latter drops to 0.08 with a b-tagging efficiency of 43%. Note that our analysis does not employ charm-tagging.

The p_T cuts on the charm quarks have a most significant impact on the event rate, see Tab. I. The number of reconstructed stops with a long life then depends strongly on the stop-neutralino mass splitting. Assembling all factors and neglecting further detector effects, up to ~ 100 events can be expected for $10\,\text{fb}^{-1}$ at our

p_T^{min}	30 GeV	35 GeV	40 GeV	50 GeV
$\Delta m = 5$ GeV	0.4%	0.2%	0.08%	0.02%
$\Delta m = 10$ GeV	7%	4%	2%	1%
$\Delta m = 15$ GeV	18%	13%	9%	4%
$\Delta m = 30$ GeV	45%	38%	32%	22%

TABLE I: The fraction of events of processes Eq. (4) with both charm quarks surviving a p_T cut for different values of p_T^{min} and Δm for $m_{\tilde{t}} = 100$ GeV and $m_{\tilde{g}} = 500$ GeV.

benchmark point at the LHC.

IV. LONG-LIVED STOP AND GRAVITINO LSP

So far we did not make use of an LSP-feature of the lightest neutralino. We only assumed tacitly that the χ^0 is stable on the size of the detector. We ask now about the implications for the stop decay length analysis outlined in the previous section if the gravitino $\tilde{G}$ is the LSP.

Interactions of the gravitino with the other MSSM particles are down by the reduced Planck mass $m_{\rm Pl} = 1/\sqrt{8\pi G_N} = 2.4 \cdot 10^{18}$ GeV and typically yield very slow decays. This suppression can, however, be lifted with small masses $m_{3/2}$ of the gravitino due to its goldstino component. Indeed, gravitino masses are linked to the susy breaking F-terms, $m_{3/2} = F/(\sqrt{3} m_{\rm Pl})$, and can be very low, even below eV, depending on the mediation mechanism, see *e.g.,* [5] for a brief overview and references therein.

We consider two cases: In the first one, discussed in Sec. IV A, the lighter stop is the NLSP. In the second scenario, addressed in Sec. IV B, we assume $m_{\tilde{t}} > m_{\chi^0} > m_{3/2}$ such that the stop can decay to both the gravitino and the lightest neutralino, which is the NLSP. The full decay chain $\tilde{t} \to c\chi^0 \to c\gamma\tilde{G}$ arising in the second case is discussed in Sec. IV C.

We assume that the decay $\tilde{t} \to t\tilde{G}$ is kinematically closed.

A. Stop NLSP

If the lightest stop is the NLSP, it decays directly via FCNC to the gravitino. The decay rate can be written as

$$\Gamma(\tilde{t} \to c\tilde{G}) = \frac{z^2}{48\pi} \frac{m_{\tilde{t}}^5}{m_{3/2}^2 m_{\rm Pl}^2} \left(1 - \frac{m_{3/2}^2}{m_{\tilde{t}}^2}\right)^4 , \qquad (12)$$

where $z = \sqrt{|z_L|^2 + |z_R|^2}$, and $z_L(z_R)$ denotes the coupling to left (right)-chiral charm quarks. Here we neglected the mass of the charm quark in the phase space calculation. Within MFV, the $z_{L,R}$-couplings are CKM- and Yukawa-suppressed as

$$z_L \propto \lambda_b^2 V_{cb} V_{tb}^*, \quad z_R \sim \lambda_c z_L \ll z_L. \qquad (13)$$

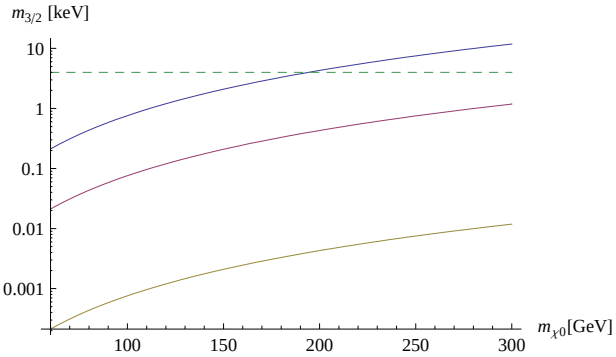

FIG. 7: Contours of fixed χ^0 lifetimes in the m_{χ^0}-$m_{3/2}$ plane as in Eq. (15). The solid curves correspond, from top to bottom, to $c\tau_{\chi^0} = 10\text{m}, 10\text{cm}, 10\mu\text{m}$. The dashed line indicates the warm dark matter constraint $m_{3/2} > 4\,\text{keV}$ [22].

Evaluating Eqs. (12)-(13) for a gravitino with mass not much lower than the one of the lighter stop to ensure dominance of the FCNC over the tree level four-body $\tilde{t} \to b\ell\nu\tilde{G}$ decays, one finds that the stop always leaves the detector undecayed, *i.e.,* the proper decay length is larger than ~ 10 m. Again, this is ruled out for light stops with mass below 249 GeV by CDF [21].

We conclude that in the light stop NLSP scenario with a gravitino LSP, there will not be a decay length measurement indicative for the flavor properties of the susy breaking from charm plus missing energy inside the detector.

B. Neutralino NLSP

In the presence of a gravitino with mass below m_{χ^0}, the lightest neutralino can decay via $\chi^0 \to X\tilde{G}$, where X can be the photon or the Z-boson or a neutral Higgs. While the estimation of the exact NLSP lifetime depends on its composition and, if higgsino components are present, on the presently unknown Higgs masses and mixing angles, we ask here under which circumstances the χ^0 decays inside of the detector.

Assuming a significant bino/wino fraction in the χ^0, the gravitino decay rate can be written as [5]

$$\Gamma(\chi^0 \to \gamma\tilde{G}) \simeq \frac{1}{48\pi} \frac{m_{\chi^0}^5}{m_{3/2}^2 m_{\rm Pl}^2} + \mathcal{O}\left(\frac{m_{3/2}^2}{m_{\chi^0}^2}\right), \qquad (14)$$

yielding lifetimes for the lightest neutralino as

$$\tau_{\chi^0} \simeq 10^{-6} s \left(\frac{100\,\text{GeV}}{m_{\chi^0}}\right)^5 \left(\frac{m_{3/2}}{4\,\text{keV}}\right)^2 . \qquad (15)$$

This constitutes a lower bound on τ_{χ^0} because the decay rates to the massive bosons are further phase space suppressed.

In Fig. 7 we show contours of fixed χ^0 lifetimes in the m_{χ^0}-$m_{3/2}$ plane calculated according to Eq. (15). The

three solid curves (from top to bottom) indicate the regions below which the χ^0 decays inside of the detector ($c\tau_{\chi^0} = 10$m), above which a secondary vertex may be observed directly ($c\tau_{\chi^0} = 10$cm), and below which the decay appears to be prompt ($c\tau_{\chi^0} = 10\mu$m). Here we ignored effects from the parent stop decay length, which push the solid curves to lower gravitino masses. Higgsino admixture and subdominance of decays to photons, hence a longer χ^0 lifetime, will shift all solid curves downward as well. Also shown in Fig. 7 is the lower bound on the gravitino mass $m_{3/2} > 4\,\text{keV}$ obtained from assuming that the gravitino is responsible for the observed warm dark matter density in the universe [22] (dashed line).

The lighter stop can also decay directly to the gravitino. We use $\tilde{t} \to bW\tilde{G}$ with subsequent decay of the W-boson into two light SM fermions as an estimate for multi-body final states. In the limit where the charginos and all squarks except for the NLSP are heavy and the gravitino is light, the decay rate for $\tilde{t} \to bW\tilde{G}$ can be written as [23], within MFV,

$$\Gamma(\tilde{t} \to bW\tilde{G}) = \frac{\alpha|V_{tb}|^2}{384\pi^2 \sin^2\theta_W} \frac{m_{\tilde{t}}^5}{m_{3/2}^2 m_{\rm Pl}^2} \times \left[|c_L^2|\, I\Big(\frac{m_W^2}{m_{\tilde{t}}^2}, \frac{m_t^2}{m_{\tilde{t}}^2}\Big) + |c_R^2|\, J\Big(\frac{m_W^2}{m_{\tilde{t}}^2}, \frac{m_t^2}{m_{\tilde{t}}^2}\Big) \right]. \quad (16)$$

Here m_W denotes the mass of the W-boson, and $c_L(c_R)$ parametrizes the amount of the lighter stop's $\tilde{t}_L(\tilde{t}_R)$-content, *e.g.,* [5], which is not fixed by requiring MFV. Up to small effects from intergenerational squark mixing is $|c_R^2| + |c_L^2| = 1$. The phase space functions I and J are given in [23].

Comparing Eq. (16) to Eq. (3), one finds that for

$$m_{3/2} \gtrsim \begin{pmatrix} 0.3 \\ 24 \end{pmatrix} \text{meV} \left(\frac{5 \cdot 10^{-7}}{Y \Delta m / m_{\tilde{t}}} \right), \; m_{\tilde{t}} = \begin{pmatrix} 100 \\ 150 \end{pmatrix} \text{GeV}, \quad (17)$$

FCNC stop decays into the lightest neutralino are more rapid than those directly into the gravitino. The above bound on the gravitino mass stems from assuming a purely right-handed lightest stop. A left-handed $\tilde{t}$ or left-right admixture allows for similar but somewhat smaller values of $m_{3/2}$ than in those in Eq. (17).

For the large splittings between the mass of the $\tilde{t}$ and the $\tilde{G}$ considered here, within MFV, the FCNC decays Eq. (12), are suppressed with respect to the ones from the charged current decays Eq. (16). Note also that for most of the parameter space, the lower limit on $m_{3/2}$ in Eq. (17) is not more constraining than the requirement of having a not too light superpartner spectrum.

We conclude that for gravitinos with mass above a few keV, the neutralino NLSP will decay outside of the detector and that our analysis for $\tilde{t} \to c\chi^0$ outlined in Sec. III is unaffected. The case of lighter gravitinos is discussed in the next section.

C. Stop pairs and energetic photon signals

Following the analysis of the neutralino lifetime of the previous Sec. IV B, a spectrum $m_{\tilde{t}} > m_{\chi^0} > m_{3/2}$ together with a very light gravitino $m_{3/2} \lesssim$ keV allows for the exciting possibility that the neutral bosons X from $\tilde{t} \to c\chi^0 \to cX\tilde{G}$ decays are seen within detectors such as those at the LHC.

We focus here on the case where X is a photon; hence, we assume a significant gaugino content in the lightest neutralino. The photons are energetic, with energies of $\sim m_{\chi^0}/2$ in the rest frame of the χ^0. (Since $m_{3/2} \ll m_{\chi^0}$, the gravitino can be taken as massless in the kinematics.)

In Fig. 8, we show the transverse momentum spectra of the photons from $\tilde{t} \to c\chi^0 \to c\gamma\tilde{G}$ with the stops pair-produced in $pp \to \tilde{t}\tilde{t}^*$ at the LHC [37]. We use $m_{\tilde{t}} = 100$ GeV and $\mathcal{B}(\chi^0 \to \gamma\tilde{G}) = 1$. We also use $\Delta m = 5$ GeV, but for $\Delta m \ll m_{\chi^0}$ the dependence of the photon spectra on the mass splitting is very mild. Note that constraints on the relevant sparticle masses and compositions from the recent CDF analysis obtained within gauge mediated susy breaking (GMSB) [25] may apply, see [26].

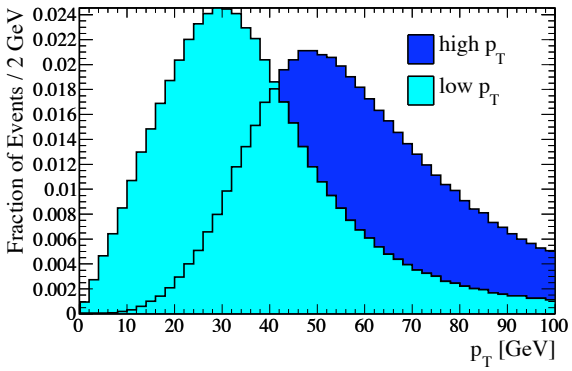

FIG. 8: The photon p_T distributions stemming from the decays $\tilde{t} \to c\chi^0 \to c\gamma \not{E}_T$ of stops produced in $pp \to \tilde{t}\tilde{t}^*$ at the LHC for $m_{\tilde{t}} = 100$ GeV. The light blue (lighter shaded) histogram corresponds to the photons with per event lower p_T.

The hard photons are a distinctive signature to efficiently suppress backgrounds [26, 27], and stop pair-production $pp \to \tilde{t}\tilde{t}^*$ becomes relevant for the LHC. While a full simulation of long-lived stops with energetic photons from NLSP decays is beyond the scope of this work, we briefly give the features of stop pair-production $pp \to \tilde{t}\tilde{t}^*$ and its impact on stop decay length measurements.

Compared to top-associated production worked out in Sec. III the boost factors of the stops from di-stop production are somewhat smaller. Numerically, the average impact parameter can be well approximated as

$$\langle b \rangle \simeq 100\,\mu\text{m} \cdot \left(\frac{\tau}{\text{ps}} \right), \quad (18)$$

which is roughly half as large as the one in top-associated stop production given in Eq. (8) and also macroscopic. In Fig. 9 we show the p_T distribution of the charm quarks

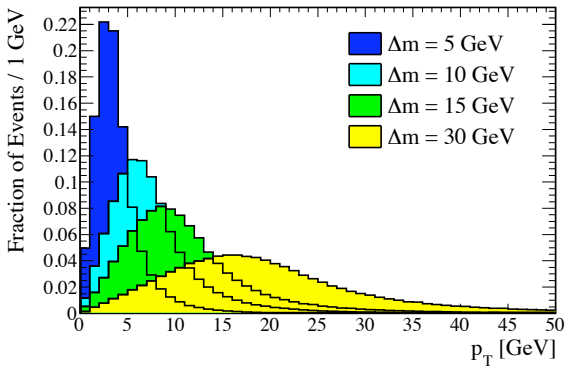

FIG. 9: The p_T distribution of the lower p_T charm quarks stemming from the decays of light stops produced in $pp \to \tilde{t}\tilde{t}^*$ at the LHC for $m_{\tilde{t}} = 100$ GeV and different mass splittings Δm.

with lower p_T arising in stop decays from $pp \to \tilde{t}\tilde{t}^*$.

The advantage of direct stop pair-production over same-sign top-associated production Eq. (4) is a substantially larger production cross section and the independence of the gluino mass, which might be heavier than a TeV. Signal loss due to stoponium formation of the di-stops with small relative momentum upon production is about a percent effect for light stops of $\mathcal{O}(100)$ GeV [28].

The photons are further useful for the stop decay length extraction and the determination of mass and mixing parameters. Independent of the stop production mechanism, the following scenarios can arise within susy with MFV:

- The $\tilde{t}$ gives a secondary vertex, and the photon points at it. The prompt NLSP-χ^0 decay yields an upper bound on its lifetime and on the gravitino mass of the order $m_{3/2} \lesssim \mathcal{O}(10)$ eV, see Fig. 7. The secondary stop decay vertex can be reconstructed using three handles: the charm jet, the stop track, and the pointing photon.

- The $\tilde{t}$ gives a secondary vertex, and the photon originates from a tertiary vertex. The χ^0 decay length is informative of the gravitino mass and the neutralino mass and admixture. Approximately, the gravitino mass ranges between a few 0.01 keV and a few keV, see Fig. 7. The bound on $m_{3/2}$ gets lowered with higgsino admixure in the lightest neutralino and also with large χ^0 boosts.

- The $\tilde{t}$ decays before reaching the innermost layer of the detector. A finite impact parameter $b \neq 0$ from charm is observed. The χ^0 decays before reaching detector material. The upper bound on the decay length of the χ^0 implies $m_{3/2} \lesssim 1$keV, see Fig. 7.

- The $\tilde{t}$ decays before reaching the innermost layer of the detector. A finite impact parameter from charm is observed. The production vertex of the energetic photon is seen. It can be used to give an upper bound on the lifetime of the χ^0. The range for the gravitino mass is as in the second scenario.

Photons in ATLAS/CMS can be seen in the calorimeter and as converted photons in the tracker. LHC studies exist for promptly produced NLSPs decaying to gravitinos with non-pointing photons [29] and prompt photons [30]. Also see [31] for a Tevatron study with promptly decaying stops.

V. SUMMARY

After measuring the parameters responsible for quark flavor violation in the SM, it is even more obvious to ask about the flavor quantum numbers of the SM partners related to electroweak symmetry breaking at TeV-energies. We elaborate here on the prospects of a decay length measurement that probes the amount of flavor violation of susy breaking couplings in the squark sector at the LHC.

Generically, a light stop is long-lived only if flavor is broken minimally, *i.e.*, purely by the quark Yukawa matrices. (An exception is an unstable stop LSP decaying slowly to SM fermions in models with broken R-parity.) While all such MFV models give strongly CKM-suppressed intergenerational stop mixing, whether one then sees in the decay $\tilde{t} \to c\chi^0$ an impact parameter, $c\tau \gtrsim \mathcal{O}(50\mu\text{m})$, or a track possibly with secondary vertex, $\mathcal{O}(\text{few cm}) \lesssim c\tau \lesssim 10$m, depends on the composition of the stop and its decay products. If the mass splittings and mixings are known, the decay length allows further to obtain information on the mediation mechanism of susy breaking.

Light stops are produced at the LHC with controlled backgrounds through gluinos in association with like-sign tops. We find substantial stop boost factors $\gamma\beta \sim 1 - 10$ and cross sections in the pb range for gluino masses not exceeding a TeV and stop masses around $\mathcal{O}(100)$ GeV. Depending strongly on the stop-neutralino mass difference, up to $\sim$ 100 events can be expected for $10\,\text{fb}^{-1}$ integrated luminosity.

Squark flavor violation can be probed by the stop decay length with a neutralino or a gravitino LSP as long as in the latter case the neutralino is the NLSP. If the neutralino is not the dark matter particle, the spectrum can be heavier than $\mathcal{O}(100\,\text{GeV})$ while keeping the splitting between the lightest stop and neutralino sufficiently small.

The gravitino LSP provides a further opportunity if the gravitino is very light, below a few keV. Besides posing no cosmological gravitino problem [32], in this case the energetic photon from $\tilde{t} \to \chi^0 c \to \gamma\tilde{G}c$ can be emitted inside of the detector. This additional signature is

advantageous for both the stop and the neutralino lifetime determination. It also suppresses backgrounds such that studies based on $pp \to \tilde{t}\tilde{t}^*$ with large stop production cross sections independent of the gluino mass come into reach at the LHC.

We conclude that collider searches for displaced or secondary vertices are a promising area for explorations of many aspects of TeV scale physics.

Acknowledgments

We are indebted to Laura Covi, Manuel Drees, David Morrissey, Michael Ratz and Carlos Wagner for useful discussions. This work is supported in part by the Initiative and Networking Fund of the Helmholtz Association, contract HA-101 ("Physics at the Terascale") and the German-Israeli-Foundation (G.I.F.). G.H. gratefully acknowledges the hospitality and stimulating atmosphere provided by the Aspen Center for Physics during the final phase of this work.

[1] Y. Grossman, Z. Ligeti and Y. Nir, arXiv:0904.4262 [hep-ph].
[2] A. Soni, arXiv:0907.2057 [hep-ph].
[3] G. Hiller and Y. Nir, JHEP **0803**, 046 (2008) [arXiv:0802.0916 [hep-ph]].
[4] R. Dermisek, H. Verlinde and L. T. Wang, Phys. Rev. Lett. **100**, 131804 (2008) [arXiv:0711.3211 [hep-ph]].
[5] S. P. Martin, arXiv:hep-ph/9709356.
[6] G. D'Ambrosio, G. F. Giudice, G. Isidori and A. Strumia, Nucl. Phys. B **645**, 155 (2002) [arXiv:hep-ph/0207036].
[7] K. i. Hikasa and M. Kobayashi, Phys. Rev. D **36**, 724 (1987).
[8] Y. Nir and N. Seiberg, Phys. Lett. B **309**, 337 (1993) [arXiv:hep-ph/9304307].
[9] V. M. Abazov *et al.* [D0 Collaboration], Phys. Lett. B **665**, 1 (2008) [arXiv:0803.2263 [hep-ex]].
[10] S. Kraml and A. R. Raklev, Phys. Rev. D **73**, 075002 (2006) [arXiv:hep-ph/0512284].
[11] W. Beenakker, M. Kramer, T. Plehn, M. Spira and P. M. Zerwas, Nucl. Phys. B **515**, 3 (1998) [arXiv:hep-ph/9710451].
[12] J. M. Yang and B. L. Young, Phys. Rev. D **62**, 115002 (2000) [arXiv:hep-ph/0007165]; A. Djouadi, M. Guchait and Y. Mambrini, Phys. Rev. D **64**, 095014 (2001) [arXiv:hep-ph/0105108].
[13] T. Han, K. i. Hikasa, J. M. Yang and X. m. Zhang, Phys. Rev. D **70**, 055001 (2004) [arXiv:hep-ph/0312129].
[14] M. Carena, A. Freitas and C. E. M. Wagner, JHEP **0810**, 109 (2008) [arXiv:0808.2298 [hep-ph]].
[15] T. Stelzer and W. F. Long, Comput. Phys. Commun. **81**, 357 (1994) [arXiv:hep-ph/9401258].
[16] J. Pumplin, D. R. Stump, J. Huston, H. L. Lai, P. M. Nadolsky and W. K. Tung, JHEP **0207**, 012 (2002) [arXiv:hep-ph/0201195].
[17] W. Beenakker, R. Hopker, M. Spira and P. M. Zerwas, Nucl. Phys. B **492**, 51 (1997) [arXiv:hep-ph/9610490].
[18] G. Aad *et al.* [ATLAS Collaboration], JINST **3**, S08003 (2008).
[19] R. Adolphi *et al.* [CMS Collaboration], JINST **0803**, S08004 (2008) [JINST **3**, S08004 (2008)].
[20] A. C. Kraan, Eur. Phys. J. C **37**, 91 (2004) [arXiv:hep-ex/0404001]; M. Fairbairn, A. C. Kraan, D. A. Milstead, T. Sjostrand, P. Skands and T. Sloan, Phys. Rept. **438**, 1 (2007) [arXiv:hep-ph/0611040].
[21] T. Aaltonen *et al.* [CDF Collaboration], Phys. Rev. Lett. **103**, 021802 (2009) [arXiv:0902.1266 [hep-ex]].
[22] M. Viel, G. D. Becker, J. S. Bolton, M. G. Haehnelt, M. Rauch and W. L. W. Sargent, Phys. Rev. Lett. **100**, 041304 (2008) [arXiv:0709.0131 [astro-ph]].
[23] U. Sarid and S. D. Thomas, Phys. Rev. Lett. **85**, 1178 (2000) [arXiv:hep-ph/9909349].
[24] T. Sjostrand, S. Mrenna and P. Skands, JHEP **0605**, 026 (2006) [arXiv:hep-ph/0603175].
[25] T. Aaltonen *et al.* [CDF Collaboration], arXiv:0910.3606 [hep-ex].
[26] G. Hiller, J.S. Kim and H. Sedello, in preparation.
[27] S. Shirai and T. T. Yanagida, arXiv:0905.4034 [hep-ph].
[28] M. Drees and M. M. Nojiri, Phys. Rev. D **49**, 4595 (1994) [arXiv:hep-ph/9312213].
[29] K. Kawagoe, T. Kobayashi, M. M. Nojiri and A. Ochi, Phys. Rev. D **69**, 035003 (2004) [arXiv:hep-ph/0309031].
[30] K. Hamaguchi, E. Nakamura and S. Shirai, Phys. Lett. B **666**, 57 (2008) [arXiv:0805.2502 [hep-ph]].
[31] M. S. Carena, D. Choudhury, R. A. Diaz, H. E. Logan and C. E. M. Wagner, Phys. Rev. D **66**, 115010 (2002) [arXiv:hep-ph/0206167].
[32] H. Pagels and J. R. Primack, Phys. Rev. Lett. **48**, 223 (1982).
[33] An on-shell particle with mass m moving with momentum $\vec{p}$ has energy $E = \sqrt{|\vec{p}|^2 + m^2}$, $\gamma = E/m$ and $\beta = |\vec{p}|/E$.
[34] We always assume 14 TeV center-of-mass energy unless otherwise stated.
[35] In our simulations we let the stops decay at the time t with the probability $\Gamma \exp(-t\Gamma)$. We use "lifetime" synonymous for the mean lifetime $\tau = 1/\Gamma$ throughout this work.
[36] For relativistic particles the effect of a boost-enlarged decay length is compensated by the boost-suppression of the angle between the particle and its decay products, and vice versa.
[37] We use PHYTHIA 6.4.19 [24] as a framework to calculate the decays of the neutralinos.